European Journal of Cell Biology 95 (2016) 295–310

Contents lists available at ScienceDirect

European Journal of Cell Biology

journal homepage: www.elsevier.com/locate/ejcb

Research paper

Urokinase and urokinase receptor participate in regulation of neuronal migration, axon growth and branching

Ekaterina Semina[a,b], Kseniya Rubina[a,*], Veronika Sysoeva[a], Karina Rysenkova[a], Polina Klimovich[a], Olga Plekhanova[b], Vsevolod Tkachuk[a,b]

[a] Department of Biochemistry and Molecular Medicine, Faculty of Medicine, M.V. Lomonosov Moscow State University, Lomonosovsky av. 31/5, 119192 Moscow, Russian Federation
[b] Laboratory of Molecular Endocrinology, Russian Cardiology Research Center, 3rd Cherepkovskaya 15a, 12155 Moscow, Russian Federation

ARTICLE INFO

Article history:
Received 2 April 2016
Received in revised form 27 May 2016
Accepted 31 May 2016

Keywords:
Urokinase
Urokinase receptor
3D explants of Dorsal Root Ganglia (DRG)
Axon growth
Axon branching
Neuronal migration

ABSTRACT

Purpose: Recent findings indicate the significant contribution of urokinase and urokinase receptor (uPA and uPAR) in the processes of nerve regeneration, however, their role in axonal growth and branching is unclear. Using a 3D model of mouse Dorsal Root Ganglia (DRG) explants, differentiated into neurons Neuro 2a cells and transgenic mice lacking the urokinase gene, we studied the involvement of the uPA/uPAR system in the neural cell migration, neurite outgrowth, elongation and branching.
Results: uPA and uPAR are expressed in the growth cones of axons. Using an *ex vivo* model of DRG explants in Matrigel we have found that uPA inhibition attenuates neural cell migration and axonal growth, pointing to an important role of urokinase in these processes. Apparently, uPA mediates its effects through its specific receptor uPAR: anti-uPAR antibody, which blocks the uPA binding to uPAR, stimulates axon branching and attenuates neural cell migration from DRG explants. Simultaneous inhibition of uPA and uPAR almost completely prevents the axonal outgrowth from explants into the Matrigels. Experiments *in vitro* using Neuro 2a cells differentiated into neurons demonstrate that administration of exogenous uPA increases the neurite growth rate (elongation), most likely via the interaction of uPA with uPAR. Blocking of uPAR stimulates neurite formation and enhances branching of preexisting neurites. The results obtained on DRG explants from transgenic mice lacking uPA gene support the assumption that uPA stimulates neurite growth via uPA/uPAR interaction and uPAR role in axons branching and neural cell migration.
Conclusions: The uPA/uPAR system plays an essential role in neural cell migration, axonal growth and branching.

1. Introduction

The urokinase system is important for plasminogen activation and fibrinolysis. The urokinase system comprises urokinase (uPA), a serine protease that cleaves and activates inactive zymogen plasminogen to the active endopeptidase plasmin, and uPAR—uPA high affinity receptor. uPA consists of the receptor-binding N-terminal epidermal growth factor-like domain (GFD), C-terminal proteolytic domain and kringle domain. GFD domain is responsible for a highly specific uPA binding to uPAR, while kringle maintains uPA-uPAR complex stabilization and its interaction with the extracellular matrix. uPAR contains three homologous domains and is anchored to the plasma membrane via the GPI-anchor (Collen, 1999; Blasi and Sidenius, 2010). GPI-anchor provides high lateral mobility within the membrane which is important for uPAR functioning since it mediates the uPA/uPAR complex clustering at the leading edge of migrating cells and facilitates local proteolysis (Bruneau and Szepetowski, 2011). uPA binds to uPAR on the cell surface (Estreicher et al., 1989, 1990; Farias-Eisner et al., 2000), and this binding increases uPA activity (Vassalli et al., 1985). uPA in association with uPAR triggers extracellular matrix proteolysis as well as some other cellular processes (Goncharova et al., 2002; Menshikov et al., 2006a; Menshikov et al., 2006b; Kjoller and Hall, 2001).

Accumulating evidence indicates that the urokinase system is implicated in cardiovascular functioning. Previously, we have shown that uPA and uPAR are expressed in migrating and

Abbreviations: uPA, urokinase-type plasminogen activator, urokinase; uPAR, urokinase receptor; DRG, Dorsal Root Ganglia.

* Corresponding author.
E-mail address: rkseniya@mail.ru (K. Rubina).

http://dx.doi.org/10.1016/j.ejcb.2016.05.003

proliferating vascular cells and are involved in the pathogenesis of cardiovascular diseases including atherosclerosis and restenosis (Poliakov et al., 1999; Stepanova et al., 1999; Mukhina et al., 2000; Plekhanova et al., 2001, 2009). uPA promotes vascular cell migration and proliferation *via* uPA-mediated plasmin proteolysis leading to matrix degradation and growth factor activation (Blasi and Sidenius, 2010; Blasi and Carmeliet, 2002). However, uPA has non-proteolytical functions that are implemented through the rapid activation of intracellular signaling such as serine and tyrosine phosphorylation (Dent et al., 1993; Endo et al., 1998), and RhoA and Rac1 activation (Kjoller and Hall, 2001). *In vivo* local increase in urokinase content upon recombinant uPA administration or plasmid transfection greatly promotes neointima formation and inward arterial remodeling via the stimulation of the vascular cell migration, of their proliferation and of their phenotypic transformation (Poliakov et al., 1999; Stepanova et al., 1999; Mukhina et al., 2000; Plekhanova et al., 2001, 2009).

Despite the functional differences between the blood vessels and the nerves certain structural similarities could be observed (Carmeliet, 2003; Hawkins and Seeds, 1989). Vessels and nerves are aligned along each other and often have the same branching circuits in tissues. Recent findings indicate that the similarities between the nervous and the vascular system extend to the molecular level: guidance molecules and intracellular signaling that control the growing axons and their branching are used by vessels to regulate angiogenesis (Carmeliet, 2003; Hawkins and Seeds, 1989). It is known that angiogenic growth factors such as vascular growth factor (VEGF), platelet-derived growth factor (PDGF-BB), hepatocyte growth factor (HGF) and matrix metalloproteases (MMPs) that play a substantial role in angiogenesis also regulate axon growth and neuron survival (Carmeliet, 2003). On the other hand, such neurotrophins as nerve growth factor (NGF), glial cell line-derived neurotrophic factor (GDNF), brain-derived neurotrophic factor (BDNF) and membrane receptors such as tropomyosin receptor kinase B TrkB, NOTCH1 and Neiropilin-1 are required for endothelial tip cell guidance during the blood vessel growth (Carmeliet, 2003). Numerous studies provide evidence for the presence of plasminogen activators in neurons and their involvement in phenotypic change and the regulation of axon outgrowth, as well as their involvement in pathological conditions (Mukhina et al., 2000; Pittman et al., 1989; Sumi et al., 1992; Dent et al., 1993). It has been previously shown that uPAR expression is essential for the normal development of subpopulations of GABAergic neurons, since in mice with null mutation in the uPAR gene there is a selective loss of GABAergic interneurons in the brain cortex. Moreover, uPAR function may influence the migration and differentiation of parvalbumin-containing interneurons, both pre- and postnatally (Eagleson et al., 2005). uPAR mutation leads to epilepsy and an autistic phenotype in mice (Ndode-Ekane and Pitkänen, 2013). While in humans nucleotide polymorphism in PLAUR gene and its alternative ligand in the brain SRPX2 (Sushi repeat protein, X-linked 2) result in a high risk of autism disorders as well as other brain diseases (stroke and brain trauma, autism, multiple sclerosis, Alzheimer's disease, cerebral malaria, HIV-associated leukoencephalopathy and encephalitis) (Lino et al., 2014). The aforementioned data make the studies of uPAR important in understanding the mechanisms of development and functioning of neurons, as well as pointing to a possible contribution of uPAR to the pathology of the central nervous system.

In vitro studies showed that plasminogen activators are secreted by cultured peripheral neurons and Schwann cells (Krystosek and Seeds, 1984; Krystosek et al., 1988; Pittman et al., 1989). In murine embryonic DRG and in the ventral motor neurons *in vivo*, the components of the urokinase system are activated during axonal outgrowth and projection towards their peripheral targets (Franco et al., 2006; Dent et al., 1993; Seeds et al., 1996). Furthermore, in murine peripheral nerves, regenerating after a sciatic nerve cruh, the maximal axonal outgrowth correlates with a significant increase in the mRNA expression of plasminogen activators (Siconolfi and Seeds, 2001). Lino and co-authors (Lino et al., 2014) showed that during neuritogenesis uPA activates focal adhesion kinase, which is involved in the reorganization of the cytoskeleton and cell locomotion. Since uPAR is a GPI-anchored protein lacking a transmembrane part, signal transduction upon uPA binding to uPAR proceeds via lateral interaction with membrane co-receptors including integrins $\alpha5$ and $\beta1$ (Lino et al., 2014). Despite the data indicating the importance of uPA-uPAR system in neurogenesis, the role of uPA and uPAR in axon growth and branching is still unclear.

In the present study we addressed the role of the uPA-uPAR system using *in vitro* and *ex vivo* neuronal testing systems, which reflect the biological features of regeneration and repair at the whole-organism level. To identify the molecular mechanisms underlying these processes we used 3-dimensional (3D) model of neurite outgrowth from DRG explants from wild type and transgenic mice lacking the urokinase gene as well as neuroblastoma Neuro 2a cell line. In the present study we demonstrate that uPA and uPAR are essential for the regulation of axonal growth and branching as well as of neural cell migration.

2. Materials and methods

2.1. Antibodies and reagents

The following primary antibodies were used: rat anti-uPAR (cat# MAB531, RD Systems), rabbit anti-NF200 recognizing axons neurofilaments (Abcam), rabbit anti-uPA (Abcam). Secondary antibodies were anti-goat and anti-rabbit AlexaFluor® 488 or AlexaFluor® 594 (Molecular Probes). Rabbit anti-GAPDH (Santa Cruz) antibody was used in western blotting for protein loading control; HRP-conjugated donkey anti-rabbit IgG (Jackson ImmunoResearch Laboratories) was used as a secondary antibody for western blotting. The chemicals used for western blotting were from Bio-Rad, and the buffers for immunofluorescence were purchased from Gibco. Trypsin and Hank's buffer (HBSS) was purchased from Gibco. Selective uPA inhibitor (BC 11 hydrobromide) at IC_{50} 8,2 μM was purchased from Tocris Bioscience. DNA Ladder (GeneRuler 50 bp DNA Ladder) and 6X DNA Loading Dye for agarose electrophoresis were purchased from Thermo Scientific; low-melt agarose and ethidium bromide were obtained from BioRad.

2.2. Animals and ethics statement

This study was completed in accordance with the European convention for the Protection of Vertebrate Animals used for Experimental and other Scientific purposes (ETS 123). All routine procedures, including animal housing and care were conducted in accordance with the revised Appendix A to ETS 123. The study was evaluated by the local ethical committee. We used 4–5 week old male mice lacking the uPA gene (originally derived from C57/B6 mice by group of Carmeliet from the FIRC Institute of Molecular Oncology (Milan, Italy)) (Carmeliet et al., 1994) and wild type C57 male mice of matching age as a control. Mice strains were used for dorsal root ganglia (DRG) explants. Before DRG withdrawal animals were anesthetized with a lethal dose of isoflurane IsoFlo® (isoflurane, USP).

2.3. Dorsal Root Ganglia explants

For the experiment we used male mice 4–5 weeks old. Mice were anesthetized with a lethal dose of isoflurane IsoFlo® (isoflurane, USP) in a gas chamber. Other animals were exsanguinated by

decapitation. The spinal ganglia were isolated under aseptic conditions using sterile surgical instruments for small laboratory animals under a stereomicroscope Olympus SZX16. The isolated tissue was immediately placed in a Petri dish containing sterile pre-chilled Hank's buffer HBSS and transferred into the laminar flow hood. All further manipulations were performed in sterile conditions. DRGs were washed in sterile HBSS, placed in an 8-well chambered borosilicate coverglass (Lab-Tek®, cat# 155411) and covered immediately with a 60 μl drop of Matrigel (BD Matrigel™ Basement Membrane Matrix) for 3D tissue explant culture or in plates. For 2D DRG cultures, plates were covered with cold Matrigel; after Matrigel polymerization DRGs were placed on Matrigel surface (see Supplementary Fig. S1 in the online version at DOI: 10.1016/j.ejcb.2016.05.003). Wells were filled with a warm RPMI culture medium. The culture medium was replaced every 5 days. DRG explants were cultures in 5% CO_2 incubator at 37 °C.

For the suppression of endogenous uPA in DRG explants we added a specific uPA inhibitor BC 11 hydrobromide (Tocris Bioscience) at the final concentration IC_{50} 8.2 μM to the Matrigel. To block uPAR, antibodies blocking the receptor-ligand interaction (anti-uPAR antibody, R&D Systems) were used. For complete inhibition of uPA and uPAR, both blocking agents were mixed with Matrigel before placing the DRG explants and subsequent Matrigel polymerization; blocking agents were also added to the culture medium to equilibrate the system. The medium, containing the blocking agents, was changed to a fresh one every 5 days.

Visualization and imaging was carried out daily for 14 days using light microscopy (Zeiss Axoivert 2000) at low magnification. Image processing (neurite counting, measurements of neurite length, as well as the number of cells, that migrated from the explants) was performed using automated image analysis program (MetaMorph Program, Molecular Devices, PA, USA). Tissue explants from at least 3 wild type and 3 uPA-deficient mice were included in each experiment. The results of at least three independent experiments are presented.

2.4. 3-Dimensional immunofluorescent staining of DRG

To prevent Matrigel depolymerization all procedures were carried out at 37 °C. For 3-dimensional multicolor immunofluorescence staining, 8-well plates were removed from the incubator and washed with warm HBSS (Gibco). All solutions were prepared on HBSS. The samples were fixed with 4% paraformaldehyde for 24 h (Panreac). After fixation, the samples were washed in HBSS for 24 h. Next, the samples were permeabilized with 1% Triton X-100 (Triton® X-100, Peroxide Free, Panreac) for 24 h and washed in HBSS buffer for 24 h. Further, the samples were treated with 5% BSA (Sigmaaldrich), containing 1% Triton X-100, for 24 h to block non-specific binding. Then the samples were washed in HBSS containing 1% Triton X-100 for 24 h and incubated in the solution of the first antibodies for 24 h. After that the samples were washed in HBSS for 24 h, incubated in the solution of the second antibodies, and conjugated with fluorochrome AlexaFluor® 594 (1:500, Molecular Probes). Finally, the samples were placed in HBSS, containing DAPI (Sigmaaldrich, 1:10000) to visualize nuclei and incubated for 24 h. To prevent contamination, the samples were stored in HBSS solution containing 0,001% NaN_3. The number of migrating cells was evaluated after DAPI staining using confocal microscopy with subsequent analysis with an automated image analysis program (MetaMorph Program, Molecular Devices, PA, USA).

2.5. 3-Dimensional confocal imaging of DRG

Images were acquired by confocal laser scanning microscopy using a microscope system (TCS SP5, Leica) equipped with a Plan-Apo ×10, 1.40 NA objective and 543-Argon lasers lines. Imaging was performed at room temperature using Leica Type F immersion oil. DAPI and AlexaFluor® 594 fluorescence were sequentially excited using lasers with wave lengths of 405 and 594, respectively. All images were captured with the same confocal gain and offset settings. Images (1024 × 1024 pixels) were saved as TIFF files in Leica LAS software and then processed in Photoshop (version CS5, Adobe) to generate figures. Images are presented as overlap of red and blue staining. The results of at least three independent experiments are presented.

2.6. Cell culture

Mouse Neuro 2a neuroblastoma (N2a) cell line (ATCC® CCL-131™) was cultured in full growth medium containing DMEM (Hyclone) with high glucose, 10% FBS (Gibco), 1× MEM Non-Essential Amino Acids Solution (Gibco) and 1× Antibiotic-antimycotic solution (Gibco). Cells were plated at a concentration of 1×10^5 cells/ml. Cells were enrolled in the experiments before the 20th passage. Differentiation of Neuro 2a cells into neurons was induced by 24 h cell deprivation with media containing 1% FBS: full growth medium was replaced by DMEM, 1× MEM Non-Essential Amino Acids Solution (Gibco), 1× Antibiotic-Antimycotic (Gibco) and 1% FBS (Hyclone) for 24 h. 1–3 days later, the differentiated cultures of neurons were used for experiments and western blotting analyses.

To evaluate the effects of uPAR on neurite branching, N2a cells were seeded onto cell culture dishes in a rare monolayer. The cells were allowed to adhere and, after uPAR blocking, antibodies (25 μg/ml) were added to the culture medium for 24 h. As a control we used non-immune IgG in an equivalent concentration. Using a light microscope we analyzed neurites in the 6 fields of view, where cells were plated in a low-concentration and had no contacts with one another.

2.7. Tissue lysates and western blotting

DRG were placed in a mortar and immediately frozen using liquid nitrogen. After nitrogen evaporation, the tissue samples were ground by a pounder. After that, the samples were transferred to Eppendorf tubes and incubated in a lysis buffer (1 μg of tissue per 1 ml of lysis buffer containing 150 mM NaCl 1% NP-40, 50 mM Tris, pH 8,0 and protease inhibitor cocktail (Pierce)). After incubation in the lysis buffer on ice for 20 min, the samples were pipetted at least 30 times and pelleted at 15,000 rpm for 10 min. Supernatants were transferred to the new tubes and their protein concentration was measured using the Bio-Rad Protein Assay (Bio-Rad Laboratories) with bovine serum albumin (BSA) as a standard.

Samples were diluted to equal protein concentration in a Laemmli buffer containing β-mercaptoethanol, heated for 10 min at 90 °C, electrophoresed in 10% SDS/polyacrylamide gel and electroblotted onto nitrocellulose membranes (Immobilon, Millipore). Kaleidoscope Prestained Standards (Bio-Rad Laboratories) were used as molecular weight markers. After rinsing in Tris-buffer saline (TBS: 150 mM NaCl, 50 mM Tris/HCl, pH 7.4), membranes were pre-blocked in an incubation buffer (TBS containing 5% (w/v) of delipidated milk and 0.5% Tween 20; TBSM) for 120 min. Membranes were incubated with the specific primary antibody for 24 h at 4 °C, washed with TBSM, and then incubated with secondary antibodies conjugated with peroxidase for 1 h. Membranes were finally washed in TBS containing 0.5% Tween 20 and visualized using SuperSignal West Pico Chemiluminescent Substrate (Thermo Scientific) and ChemiDoc™ XRS + System (BioRad) for blot imaging and analysis.

2.8. Neuro 2a immunofluorescent staining

N2a cells were seeded into the wells of the Nunc® Lab-Tek® Chamber Slide™ system at a low concentration (2×10^4/ml) in a full growth medium; 24 h later, the cells were differentiated into the neurons as described above. 24 h later, the slides were removed from the incubator and washed with warmed HBSS for 10 min. Cells were fixed in 4% formaldehyde, incubated with the first and second antibodies and then washed in HBSS. Staining of N2a cells for intracellular uPA was performed in permeabilizing conditions using Triton X-100 incubation (10 min, 0,1% in HBSS). The nuclei were counterstained with DAPI. Images were acquired by a confocal laser scanning microscopy system (TCS SP5, Leica) equipped with a Plan-Apo x60, 1.40 NA oil objective and 488- and 543-Argon lasers lines. Imaging was performed at room temperature using Leica Type F immersion oil. DAPI, AlexaFluor® 488 and AlexaFluor® 594 fluorescence were sequentially excited using lasers with wavelengths of 405 (DAPI), 488 (AlexaFluor® 488) and 594 (AlexaFluor® 594). All images were captured with the same confocal gain and offset settings.

Images (2048 × 2048 pixels) were saved as TIFF files in Leica LAS software and then compiled in Photoshop (version CS5, Adobe). The results of at least three independent experiments are presented.

2.9. HEK293 transfection

To obtain murine uPA, HEK293 cells (ATCC® CRL-1573™) were transfected with pcDNA3.1 (Life Technologies) vector, containing the full length of mouse uPA (pcDNA3.1-uPA). For a control we used conditioned media from HEK293 cells transfected with pcDNA3.1, containing the antisense sequence of luciferase. Cells were cultured in DMEM (Hyclone), supplemented with 10% FBS (Hyclone), 1× antibiotic-antimycotic solution (Gibco). For plasmid transfection Lipofectamine2000 (Life Technologies) was used, and the transfection was carried out according to the manufacturer's protocol. After 72 h, the conditioned medium from the transfected cells was collected, centrifuged to pellet debris, and the concentration of uPA was determined in the medium from the uPA-transfected and the control cells using ELISA Cell Sciences (cat# CSI19903A). The final concentration of uPA in conditioned media for further experiments was 10 ng/ml. Bovine serum albumin (BSA) was added to the control media for system equilibrating.

2.10. Neuritogenesis analysis and neurite growth pattern

To reveal the role of the urokinase system in neurite growth patterning we used uPAR blocking antibodies, exogenous uPA and a selective uPA inhibitor. The differentiated cultures of N2a cells were plated onto 24-well plates in a concentration of 2×10^4 cells/ml. Blocking uPAR antibodies (R&D Systems) were used in a concentration of 25 μg/ml, and non-immune IgG in the corresponding concentration were used as a control. To obtain mouse uPA, we used the conditioned medium from HEK293 cells that had been previously transfected with murine pcDNA3.1-uPA or control vector pcDNA3.1. The final uPA concentration in the conditioned medium enrolled in experiments was 10 ng/ml. For uPA inhibiting, we used the specific uPA inhibitor BC 11 hydrobromide at IC_{50} 8.2 μM. Neurite outgrowth was evaluated using a phase-contrast light microscope (Axiovert 2000, Zeiss Ltd.) with a dry 20× objective. The growing process was considered as a neurite if its length exceeded the diameter of the cell body. The effects of uPAR on the growth rate and branching of the neurites were evaluated after 24 h according to three criteria: (1) the formation of the new processes/outgrowths (*e.g.*, the number of processes in the cell); (2) the number of branch points in the forming neurite (the existence of a branching point was established if there was a branching of two or more independent neurites with visible thickening at the site of the branching); (3) the average neurite length. Every cell was subjected to neurite length analysis that was carried out using an automated image analysis program (MetaMorph Program, Molecular Devices, PA, USA) with the same parameter set for all samples. The amount of neurites/processes, neurite branching and the length of neurites were evaluated on 200 cells per well in 6 randomly chosen fields. The results of at least three independent experiments are presented.

2.11. Impedance measurement with the xCELLligence system

xCELLligence was used to evaluate the neurite outgrowth. The xCELLigence system (Roche, USA) monitors cellular events in real time and measures the electrical impedance across microelectrodes integrated into the bottom of E-Plates. The impedance measurement provides quantitative information on cell adhesion, cell number and viability. The differentiated neuroblastoma cells were removed from the culture dishes by trypsinization and pelleted by centrifugation. N2a cells were resuspended to the final concentration of 1×10^4 cells/ml in HEK293 conditioned medium containing uPA (10 ng/ml) or in conditioned medium from the control HEK cells. 1×10^4 of N2a cells in 100 μl media were seeded in E-plate wells after background measurement. The background measurement of the E-plates was performed in 100 μl of DMEM with 1% FBS for 30 min. The system was transferred to a CO_2 incubator. The E-plates were placed into the Real-Time Cell Analyzer (RTCA) station where the cell index was continuously monitored at 15 min intervals for 74 h. The impedance measurement experiment was repeated six times. The analysis of real-time data was performed with RTCA Software 1.2 (Roche, USA).

2.12. Murine uPAR overexpression and downregulation in N2a cells

To suppress native uPAR expression we used a commercially available plasmid vector encoding shRNA (uPAR shRNA Plasmid, Santa Cruz, sc-36782-SH). For overexpression we used a pN1 vector encoding full-length murine uPAR DNA (pN1-uPAR). The vector was obtained from Dr. N. Sidenius of the FIRC Institute of Molecular Oncology. Cell transfection was performed according to the Lipofectamine2000 (Life Technologies) protocol. After transfection, the cells were cultured for 8 weeks in a complete medium containing selective antibiotics: puromycin for sh-uPAR (at 2 μg/ml, Sigmaaldrich) and G418 for pN1-uPAR (at 200 μg/ml, Sigmaaldrich). Changes in mRNA expression were assessed using Real Time PCR (RT-PCR).

2.13. Quantitative real-time polymerase chain reaction analysis (RT-PCR)

The RNeasy® Mini Kit (Qiagen, Germany) was used for the extraction of total RNA from the DRG explants of wild type mice and uPA-deficient mice, as well as from N2a cells transfected with pN1-uPAR, shRNA-uPAR or the control vector. For cDNA preparation 1 μg of total RNA was used. The cDNA synthesis was carried out using SuperScript® III First-Strand Synthesis SuperMix for qRT-PCR (Thermo Fisher Scientific). The concentration of undiluted cDNA in qPCR reaction volume was 8%. To select the specific sequence primer, Primer-BLAST software was used following by pre-validation of the primer specificity with OligoAnalyzer 3.1 (available online at www.https://eu.idtdna.com/calc/analyzer). Further primers for murine uPAR and β-actin (used as an endogenous control gene) were obtained from Evrogen (Russia): uPAR-forward 5′-CGCCACAAACCTCTGCAAC-3′, uPAR-reverse 5′-CTCTGTAGGATAGCGGCATTG-3′, β-actin-

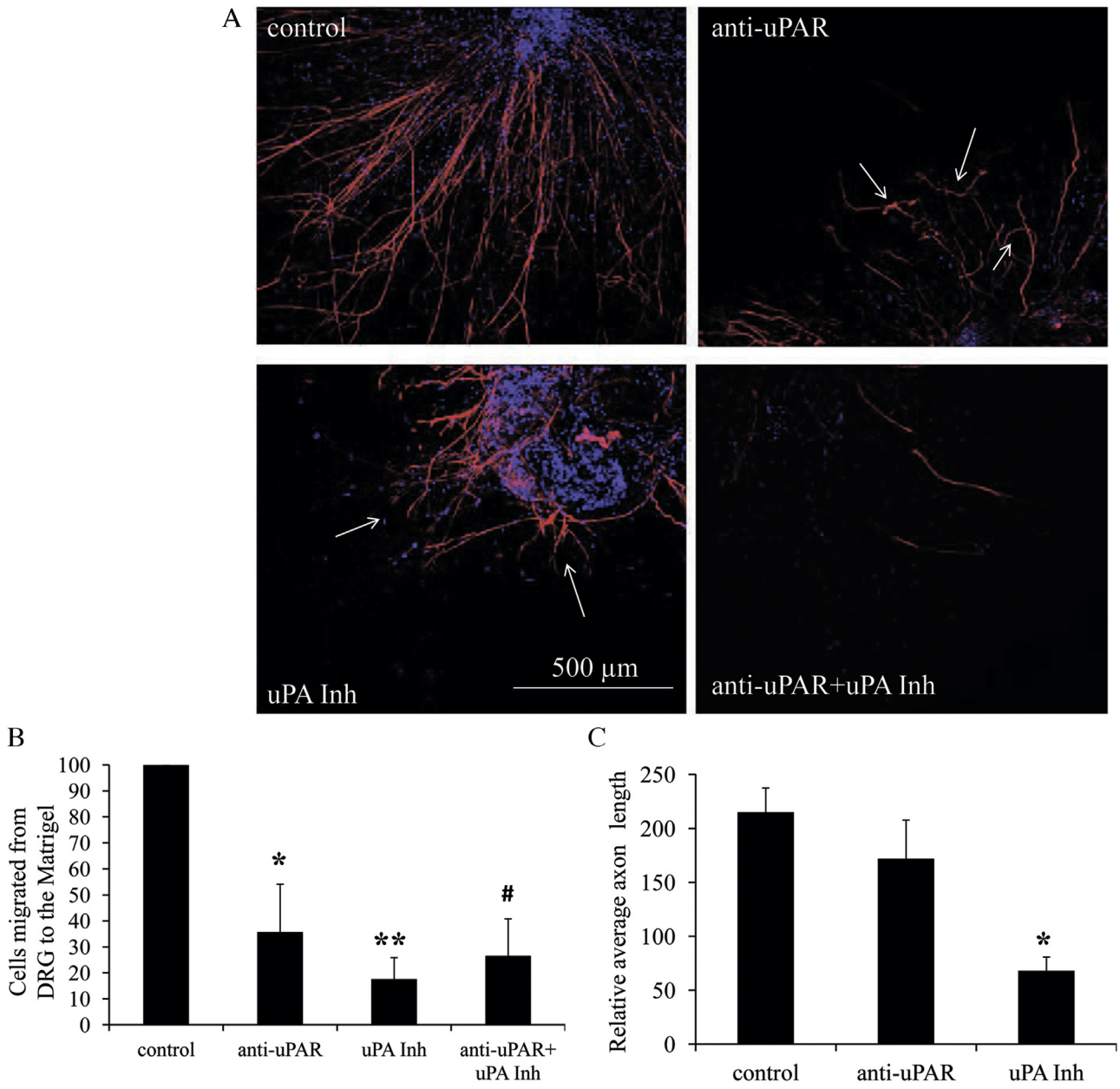

Fig. 1. uPA and uPAR affects neurites outgrowth and cell migration from DRG explants *ex vivo*. (A) After 14 days in Matrigel culture, 3D explants were stained with antibody against NF200 to visualize axons. The nuclei of cells migrated from DRG to the Matrigel were counterstained with DAPI. In control numerous radially growing axons as well as a great number of cells migrating from DRG explant could be observed. uPAR blocking by antibodies (anti-uPAR) changed the trajectory of the growing axons from a straight line to a wavy line (arrows in the figure), accompanied by the increased axonal branching. In addition, anti-uPAR reduced the migration of cells from explant to Matrigel. uPA inhibition (uPA Inh, BC 11 hydrobromide, IC_{50} 8,2 μM) led to the reduction of the number of the growing axons, a decrease in their growth rate and a distorted growth trajectory (arrows in the figure). Complete inhibition of both uPA and uPAR caused nearly total suppression of neurite outgrowth from DRG explants to Matrigel. Bars 500 μm. (B) Migrating neural cells were evaluated by the number of DAPI-stained cells outside the DGR explants. Data are shown as mean ± SEM, *,**$p < 0.05$ compared to control, #$p < 0.01$ compared to control, N = 6. (C) Assessment of the relative average length of axons emerging from DGRs into Matrigels. Data are shown as mean ± SEM, * $p < 0.001$ compared to control. Reproducible results of six independent experiments are presented.

forward 5′-AGTGTGACGTTGACATCCGTA-3′, β-actin-reverse 5′-GCCAGAGCAGTAATCTCCTTCT-3′. The primers' specificity was confirmed initially by an analysis of melting curves (raw data in Supplementary Fig. S2 in the online version at DOI: 10.1016/j.ejcb.2016.05.003) and then followed by agarose gel electrophoresis to verify the production of a single gene-specific product (Fig. 6A). The raw data of RT-PCR analysis of uPAR mRNA expression was performed using the qPCRmix-HS SYBR (Evrogen, Russia) on DT-96 real-time PCR device (DNA-technology, Russia). The raw data of RT-PCR analysis of uPAR expression are presented in Supplementary Fig. S3 in the online version at DOI: 10.1016/j.ejcb.2016.05.003. The thermal cycling program for template denaturation, uPAR and β-actin primers annealing and primer extension was 94° C for 15 s, 62° C for 15 s and 72° C for 20 s for 40 cycles, correspondingly. A relative transcript level of uPAR was calculated using the $2^{-\Delta\Delta Ct}$ method.

2.14. Statistical processing of results

Data from all experiments are presented as mean ± SEM. Comparisons between multiple groups were performed using the One-Way ANOVA and the Student-Newman-Keuls Test for mul-

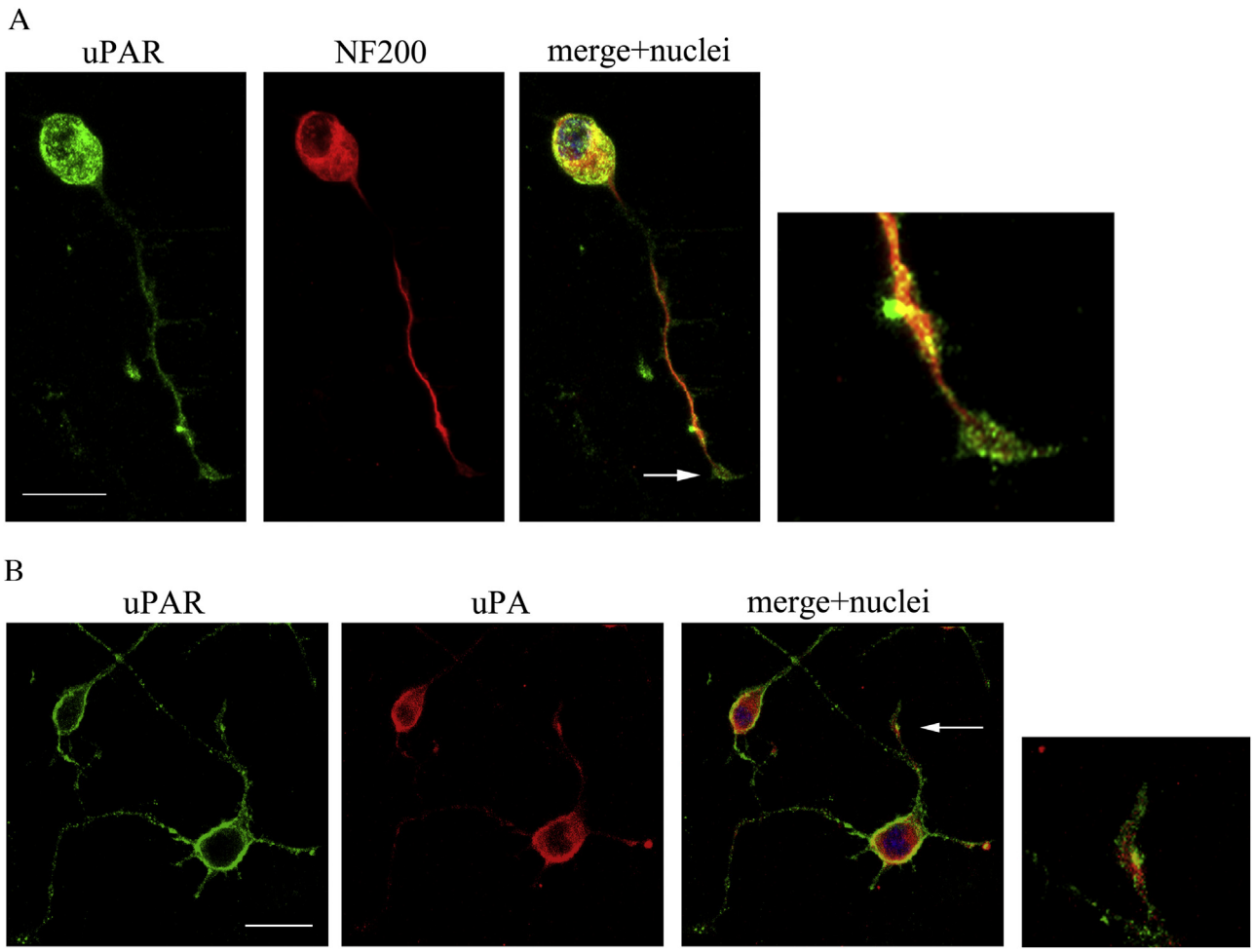

Fig. 2. Expression of uPA and uPAR on the axon growth cones in differentiated N2a cells *in vitro*. (A) Double immunofluorescent staining of N2a cells for uPAR and axon visualization (NF200). Nuclei were counterstained with DAPI. Arrows point to the growth cones. Inserts on the right depict the growth cones with higher magnification. Bars 10 μm. (B) Cells were permeabilized with 0.1% Triton X-100 and stained with antibodies against uPA (red) and uPAR (green). Nuclei were counterstained with DAPI. Arrows point to the growth cones. Inserts on the right shows the growth cones at higher magnification. Bars 10 μm. Reproducible results of three independent experiments are presented. (For interpretation of the references to colour in this figure legend, the reader is referred to the web version of this article.)

tiple comparisons. Single comparisons were made using Student's *T*-test. A value of $p < 0.05$ was considered statistically significant. The statistical analysis was performed using STATISTICA software.

3. Results

3.1. Simultaneous inhibition of uPA and uPAR abrogates axon outgrowth and cell migration from DRG explants

To study the effects of uPA and uPAR on neural cell migration and neuritogenesis we isolated dorsal root ganglia (DRG) from wild-type C57/B6 mice and cultured them inside the Matrigel drops *ex vivo*. Supplementary Fig. S1 in the online version at DOI: 10.1016/j.ejcb.2016.05.003 shows that in contrast to the 3D DRG culture, where cell migration and neurites' outgrowth from DRG into the Matrigel could be evaluated, no neurite outgrowth could be detected in the 2D DRG culture. Thus, the 3D explant DRG culture is a more relevant model than a 2D culture since it adequately reflects the *in vivo* biological features of regeneration, *i.e.* the outgrowth of neurites and the migration of neural cells.

For the selective suppression of endogenous uPA in DRG explants we added a specific uPA inhibitor BC 11 hydrobromide. To block uPAR, antibodies which block the binding of uPA to its receptor uPAR were used. For complete inhibition of uPA and uPAR, both blocking agents were mixed with Matrigel before placing the DRG explants and Matrigel polymerization. On the 14th day the DRG explants in 3D Matrigel culture were stained with antibodies recognizing mature axons (NF200) and with DAPI to visualize the nuclei of migrating cells. 3D-Matrigels with DRG explants were analyzed using a scanning confocal imaging microscope.

In control DRG explants, axons grew in a radial manner from the ganglia with minimal branching (Fig. 1A, C). Also, a large number of cells migrated outwards from the explants into the Matrigels (Fig. 1B). The suppression of endogenous urokinase (uPA Inh) substantially abrogated the axonal growth (Fig. 1A, C): the length of axons was decreased while their normal growing trajectory was impaired (arrows in Fig. 1A). Also uPA inhibition significantly reduced the number of cells that migrated from DRG explants to the Matrigels (Fig. 1B). Supplementary materials contain videos of stereomicroscopy images obtained using 3D DRG explants and presented in Fig. 1A (Video S1–S4 in the online version at DOI: 10.1016/j.ejcb.2016.05.003).

uPAR blocking led to alteration of the normal axonal growth trajectory and increased branching (arrows in Fig. 1A), however, it had no statistically significant effect on axons' length (Fig. 1C). The number of the growing axons was also reduced, as well as the

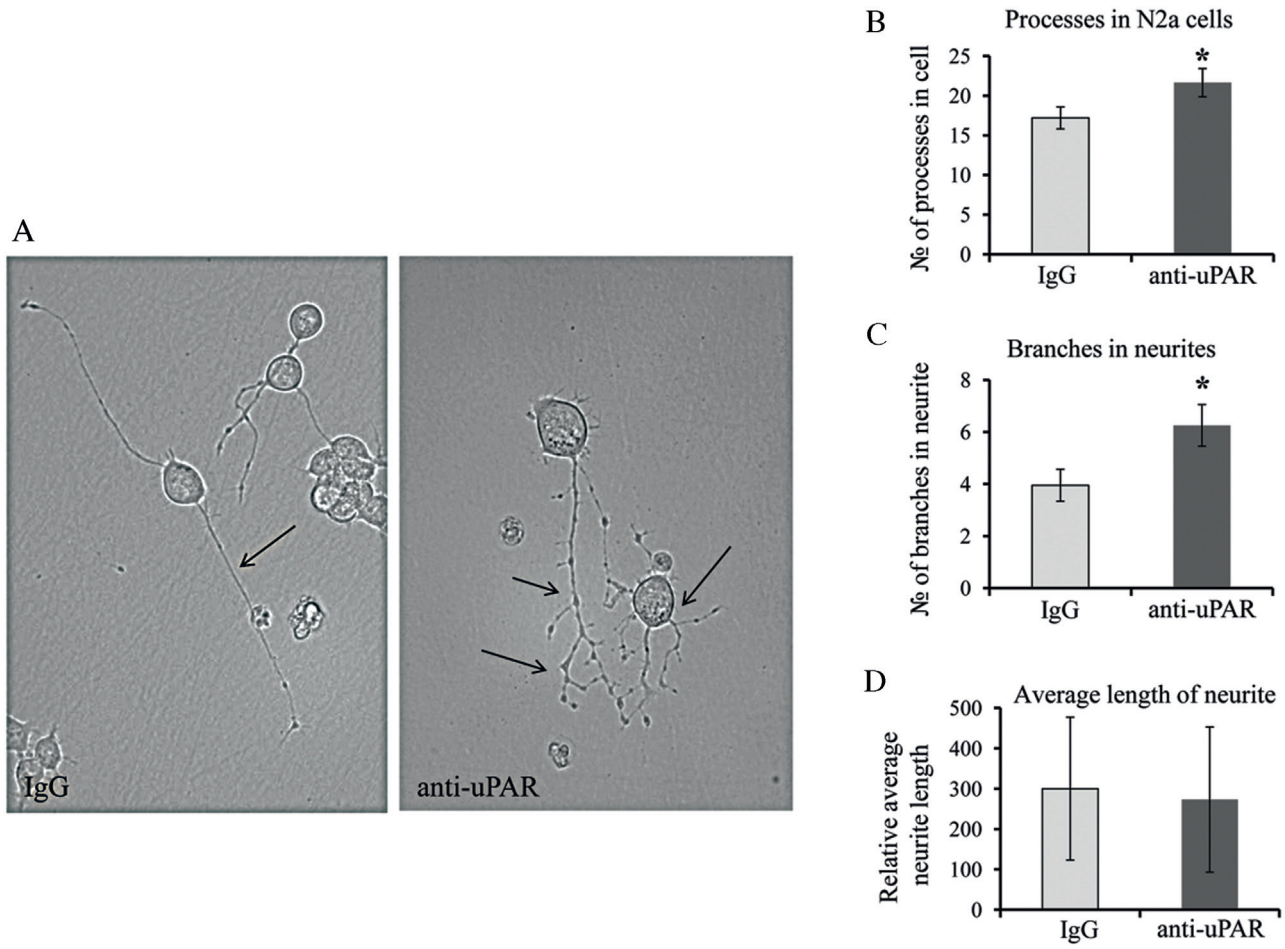

Fig. 3. uPAR blocking in neurons results changes in N2a cell morphology. Differentiated N2a cells were plated at a low cell density in culture dishes. After the cells adhered, uPAR blocking antibodies (anti-uPAR) or control IgG were added. After 24 h the cells were visualized using a light microscope (A). The number of processes, the number of branches and the length of neurites were calculated in at least 6 fields of view in each well (3 wells with anti-uPAR and 3 wells with IgG). The statistically assessed effects of uPAR blocking on the process formation, the branching (branches) and the length values (length) of neurites are presented in graphs in B–D. Data are shown as mean ± SEM, $^{*}p < 0.05$. Reproducible results of three independent experiments are presented. The arrows point to neurites in the control and neurite branching upon uPAR blocking (anti-uPAR).

number of cells migrating from explants to Matrigel decreased dramatically as assessed by the number of DAPI-stained cells around DGR explants (Fig. 1B). Surprisingly, simultaneous inhibition of uPA and uPAR almost completely suppressed the axon outgrowth from the explants (Fig. 1A). Nevertheless cell migration from explants was partially retained (Fig. 1B).

Thus, using the explant culture of mouse spinal ganglion in Matrigel, we demonstrated that uPA and uPAR was important for the axonal growth and branching as well as for the neural cell migration. Urokinase was critical for axon growth rate and cell migration, while the urokinase receptor was important for the regulation of axonal branching, their directed growth, and neural cell migration.

3.2. Blocking of uPAR stimulates neurite branching in neurons differentiated from neuroblastoma Neuro 2a cells

To investigate further the effects of urokinase system on the growth and branching of axons, we used Neuro 2a neuroblastoma cell line (N2a). N2a is a mouse neural crest-derived cell line that has been widely used to study neuronal differentiation, axonal growth and signaling pathways due to their ability to differentiate into neurons within a few days.

3.2.1. Expression of uPA and uPAR in Neuro 2a cells differentiated neurons

Neuro 2a cell differentiation was induced by cell deprivation. First, we evaluated the expression of uPA and uPAR in the growth cones of axons upon N2a differentiation. Double immunofluorescence staining of N2a cells with antibodies against NF200 and uPAR is shown in Fig. 2A. To reveal the intracellular localization of uPAR and uPA we performed the staining with uPAR and uPA antibodies after Triton X-100 permeabilization (Fig. 2B).

The immunofluorescent assay showed that differentiated cells expressed uPA and uPAR (Fig. 2). Positive staining of uPAR was detected in the soma of neurons and in their axons; it is notable that uPAR was strongly expressed in axon growth cones (shown by the arrow in Fig. 2A, B). Urokinase expression was detected in the cell body and in axon growth cones as revealed by the staining after permeabilization (shown by the arrow in Fig. 2B).

3.2.2. Neurite formation and branching depend on uPAR activity in differentiated Neuro 2a cells

We next tested if uPAR function is important for neurite formation, growth rate and branching. After cells adhered, uPAR blocking antibodies were added to the cell culture media. 24 h later using a light microscope we analyzed neurite formation in the areas where single cells located separately not touching each other.

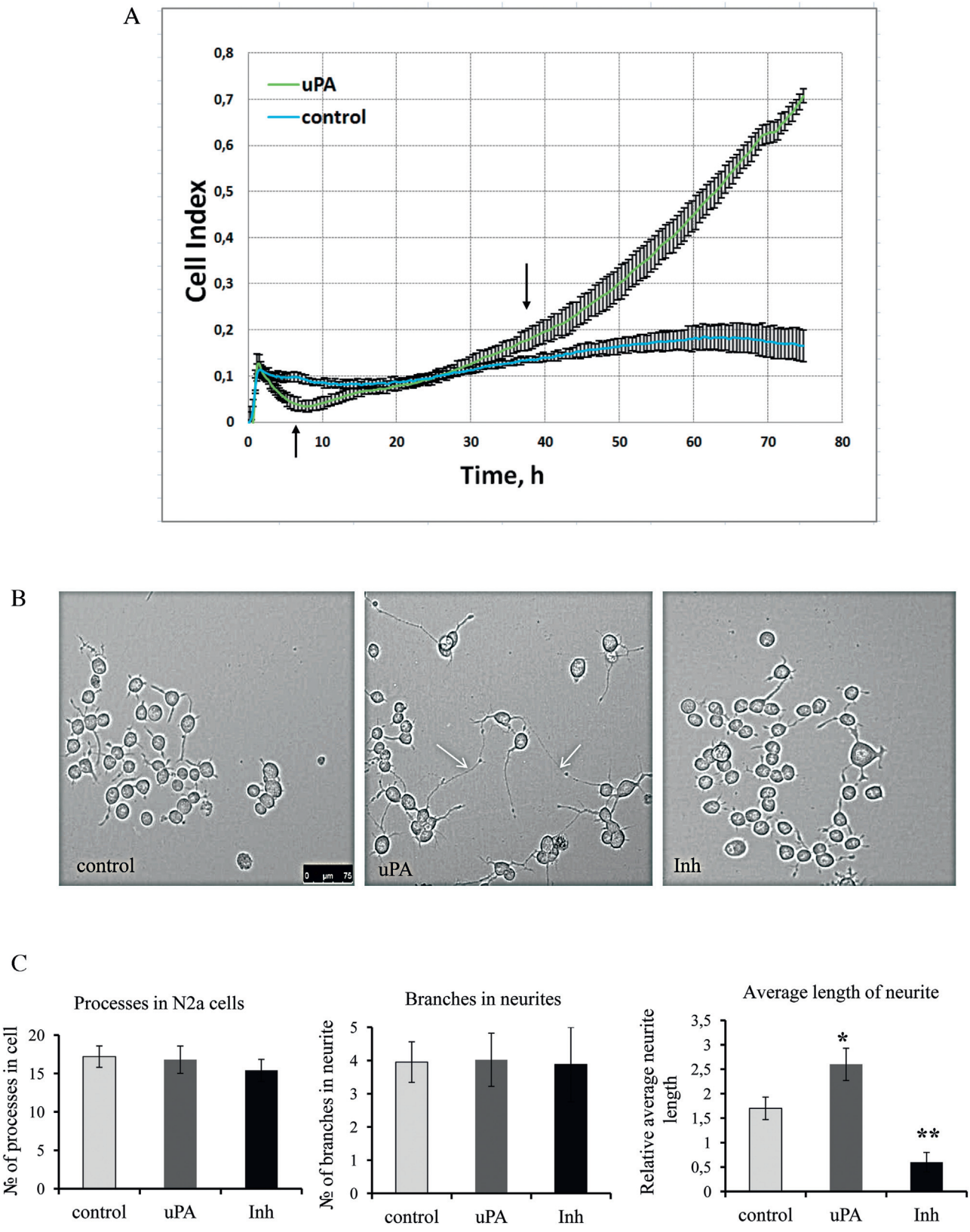

Fig. 4. The effect of urokinase on Cell Index and neurite outgrowth. (A) Cell index measurement by the xCELLigence System was automatically recorded in real time. The differentiated N2a cells were plated 10,000 cells per E-plate well. Murine uPA was added to DMEM culture media at final concentration 10 ng/ml and DMEM containing 10 ng/ml BSA was used as a control. Cell indexes were monitored for 74 h after uPA or BSA administration. All data presented are mean values of six experiments ± SEM. Left arrow indicates a statistically significant difference between the control and the uPA group after 6 h of incubation (*$p < 0.05$), right arrow indicates statistically significant differences in the cell indexes between the control and the uPA group after 35 h in culture (*$p < 0.05$). (B) The differentiated N2a cells were plated at 1×10^4/well in 6-well plates. After cell adhesion, the cell culture medium was replaced by a conditioned medium containing uPA (10 ng/ml), or by control media (BSA, 10 ng/ml) or by medium containing a uPA inhibitor (Inh, IC_{50} 8,2 μM). After 24 h the series of microphotographs was taken at least in 6 fields of view. Arrows in the figure point to long

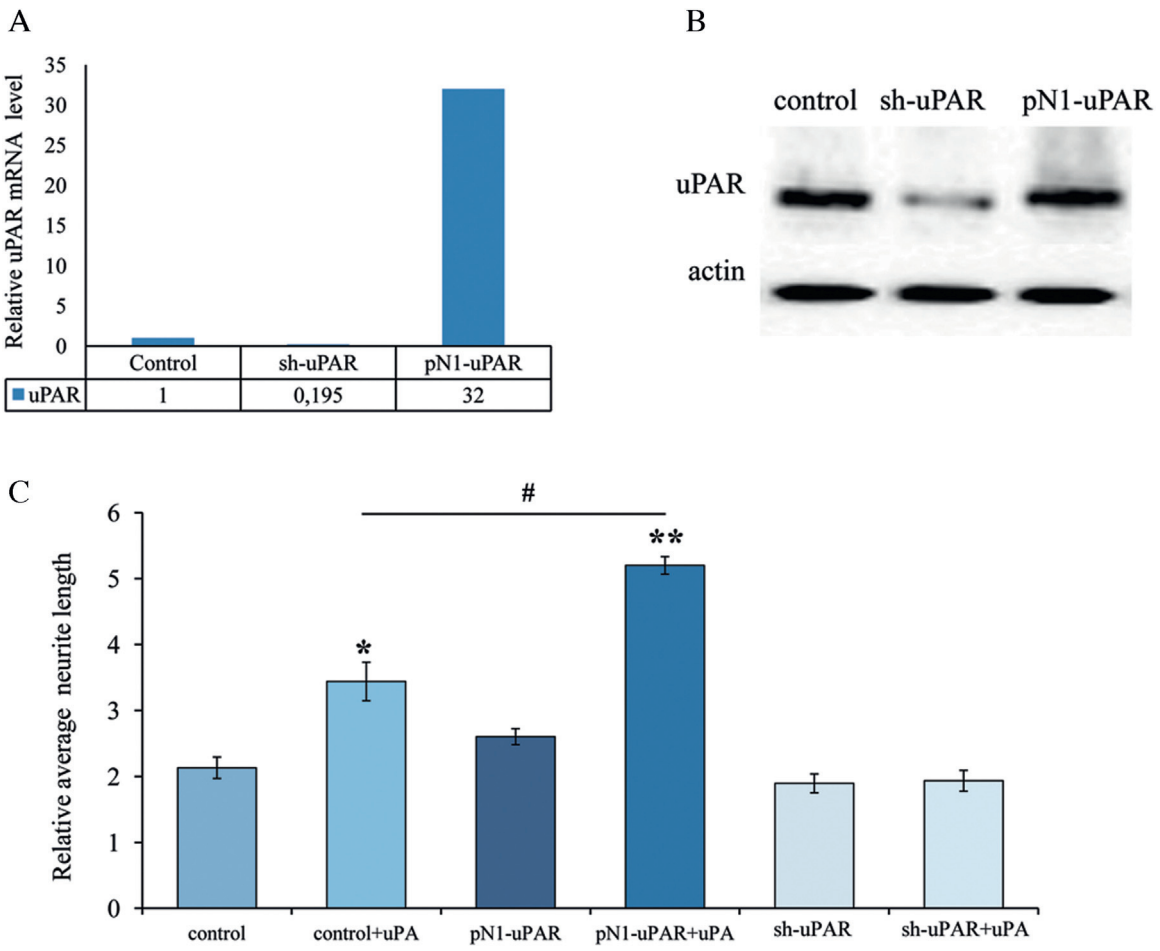

Fig. 5. Urokinase increases neurite length through interaction with uPAR in N2a cells. (A) Expression of uPAR in differentiated N2a cells. RT-PCR was carried out to evaluate the expression of uPAR in N2a control cells, in N2a cells after transfection with shRNA-uPAR and subsequent subclonal selection (sh-uPAR), and in N2a cells after transfection with pN1-uPAR (pN1-uPAR) with subclonal selection. The mRNA level was normalized to β-actin expression as a housekeeping gene. Reproducible results of three independent experiments are presented. (B) Western blot analysis of uPAR content in sh-uPAR and pN1-uPAR cells. Reproducible results of three independent experiments are presented. (C) The uPA-dependent neurites' outgrowth was measured in sh-uPAR, in pN1-uPAR cell cultures and in cells with native uPAR expression ("control"). The relative average length of the neurites was calculated using microphotographs of 6 random fields of view in each experiment. Data are shown as mean ± SEM, * indicates $p < 0.05$ between control and control + uPA; ** indicates $p < 0.01$ between pN1-uPAR and pN1-uPAR + uPA and # indicates $p < 0.005$ between control + uPA and pN1-uPAR + uPA. Reproducible results of three independent experiments are presented.

uPAR blocking led to changes in neurite growth characteristics: an increase in the average number of neurites per cell compared to the control and in a 1.5-fold increase in neurite branching. These results were statistically significant (Fig. 3, $p < 0.05$). uPAR blocking had no effect on the average neurite length of N2a cells ($p \square 0.05$). In this study we demonstrate for the first time that uPAR expression in axon growth cones is essential for normal axon growth trajectory, since uPAR blocking enhances neurite formation de novo and branching.

3.2.3. *Urokinase stimulates neurite outgrowth in Neuro 2a cells*

Based on our data obtained *ex vivo*, we hypothesized that exogenous urokinase can stimulate neurite outgrowth. Taking into account the well-established fact that urokinase promotes cell adhesion and proliferation, we assumed that uPA can also stimulate neurite outgrowth. To prove this we used xCELLligence system.

Murine uPA was obtained from HEK293 cells, which were transfected with plasmid vector for uPA expression. The conditioned medium from these cells was used as a source of exogenous uPA. We observed that during the first 2–8 h, uPA (10 ng/ml) significantly decreased the cell index compared to the control (BSA, 10 ng/ml), reflecting the reduced cell adhesion and spreading (left arrow in Fig. 4A). After 35 h a statistically significant increase in the cell index was detected, indicating that later on urokinase had a stimulatory effect on neurite outgrowth and increased their length ($p < 0.05$, right arrow in Fig. 4A). uPA administration had no statistically significant effect on neuron proliferation (data not shown).

The results obtained with xCELLigence system were confirmed by direct calculation of the length of neurites formed by N2a cells after administration of exogenous urokinase or selective uPA inhibitor (Fig. 4B). After 24-h incubation, cells were analyzed and images were taken (at least 6 fields of view for each well). The length and number of neurites was further assessed using automated image analysis program (MetaMorph Program, Molecular Devices, PA, USA). Fig. 4B demonstrates differentiated N2a cells in control (BSA, 10 ng/ml) or upon exogenous urokinase

neurites formed by the cells upon uPA administration. Bars 75 μm. (C) The evaluation of neurite formation ("Processes in N2a cells"), branching ("Branches in neurites") and neurite length ("Average length of neurite") are presented in graphs, data are shown as mean ± SEM, * and ** indicate $p < 0.05$ and $p < 0.01$ compared to the control, respectively. Reproducible results of three independent experiments are presented.

administration (uPA, 10 ng/ml), or in the presence of uPA inhibitor (Inh, IC_{50}) after 24 h of incubation. uPA administration resulted in a 40% increase in the average length of outgrowing neurites (but not the number of processes and branches) compared to the control (*, $p < 0.05$ in Fig. 4C), while uPA inhibitor dramatically reduced the length of the growing neurites (**, $p < 0.01$ Inh vs. control in Fig. 4C).

Thus, these results suggest that urokinase contributes significantly to the regulation of neurite growth rate, *i.e.* urokinase stimulates neurite outgrowth and an increase in their length.

3.2.4. Urokinase stimulates neurite outgrowth in Neuro 2a cells via interaction with uPAR

Taking into consideration the results described above we assumed that urokinase could exert its effects on neurite outgrowth via interaction with its specific receptor uPAR. To confirm the assumption, we utilized an overexpression/suppression approach. Plasmid vector encoding shRNA reduced the uPAR/mRNA level at least 5-fold in N2a cells, while overexpression using pN1-uPAR vector upregulated the uPAR/mRNA level more than 30-fold. uPAR expression was verified by real time PCR (Fig. 5A) and western blot analysis (Fig. 5B). Control N2a cells, cells overexpressing uPAR and shRNA-uPAR cells were differentiated by 24 h deprivation before the experiment. To test urokinase effects, cells were resuspended in conditioned media from the control HEK293cells or HEK293 cells producing uPA (final concentration 10 ng/ml).

Cells overexpressing uPAR (pN1-uPAR) demonstrated a slightly greater average length of neurites compared to control (Fig. 5C). In cells with suppressed uPAR (sh-uPAR) the average length of neurites was decreased compared to control (Fig. 5C). However, uPA administration significantly increased the rate of neurite outgrowth in both, control cells (1.6-fold increase in control + uPA vs. control, *$p < 0.05$) and in cells overexpressing uPAR (2-fold increase in pN1-uPAR + uPA cells vs. pN1-uPAR, **$p < 0.01$). It is notable that the administration of uPA had no effect on neurite outgrowth in cells with suppressed uPAR (sh-uPAR compared to sh-uPAR + uPA cells). The data obtained on uPAR overexpressing cells upon uPA administration resulting in increased length of the forming neurites compared to control (pN1-uPAR + uPA vs. control + uPA, #$p < 0.005$) confirm the above assumption on the importance of uPA/uPAR interaction for neurite outgrowth.

Therefore, we found that uPAR blocking resulted in the increased formation of neurites *de novo* and enhanced branching of existing neurites. The addition of uPA promoted neurite elongation, presumably due to uPA interaction with its specific receptor uPAR in the growing axons.

3.3. Blocking of uPAR in DRG explants stimulates axon branching ex vivo

Further evidence that uPA/uPAR system is essential for neurite elongation and branching as well as for neural cell migration was obtained using a 3D explant model of DRG, which were isolated from wild mice (WT) or from mice lacking uPA gene (KO-uPA). Surprisingly, RT-PCR data (Fig. 6A) and western blotting analysis demonstrated that uPAR was expressed more intensively in KO-uPA DRG than in WT DRG (Fig. 6B, C), suggesting that the elevated uPAR expression in KO-uPA DRG may reflect a compensatory mechanism for the insufficient uPA maintenance; however, this speculation requires further research.

3.3.1. Urokinase stimulates neural cell migration and neurites outgrowth by uPAR in DRG explants

The role of the urokinase system in cell migration and neurite outgrowth was investigated using DRG explants from WT or transgenic KO-uPA mice, which were incubated in Matrigels with the addition of exogenous uPA (or BSA as a control) during 14 days. The average neurite length was analyzed on the 14th day using a light microscope at low magnification (Fig. 7 A). Administration of uPA significantly stimulated the neurite outgrowth in WT (*$p < 0.05$ in Fig. 7B) and KO-uPA explants (**$p < 0.05$ in Fig. 7B). Interestingly, spontaneous neurite outgrowth in KO-uPA was greater than in WT explants (***$p < 0.001$ in Fig. 7B) and the stimulatory effect of uPA on neurite outgrowth was more profound in KO-uPA explants compared to WT explants (WT + uPA vs. KO-uPA + uPA, #$p < 0.05$ in Fig. 7B).

Furthermore, we evaluated the number of cells migrating from DRG explants into Matrigels and the relative length of cell migration paths. We found that uPA administration significantly stimulated both processes: spontaneous cell migration estimated by the number of migrating cells (*, **$p < 0.05$ in Fig. 7C), and the relative length of cell migration path *i.e.* length of cell migration (*, ** $p < 0.05$ in Fig. 7D). It is notable that in DRG from KO-uPA mice, that exhibited the elevated uPAR expression, the stimulatory effect of urokinase on neural cell migration was more pronounced than in WT explants (#, *$p < 0.05$ in Fig. 7B, C), similar to the effects of uPA on the growth of neurites in DRG explants from mice lacking the uPA gene.

These results confirm our initial assumption that the stimulating effect of uPA on neural cell migration and neurite outgrowth is mediated by the uPA interaction with its specific receptor, uPAR.

3.3.2. uPA-uPAR system affects axon growth trajectory in DRG explants of transgenic mice

To further confirm our hypothesis that uPAR is involved in the growth and branching of axons, we used uPAR blocking antibodies that were mixed with Matrigels before placing the ganglia into the three-dimensional culture. We used DRGs from wild type mice (WT) and from mice lacking urokinase (KO-uPA). We expected that, due to the elevated expression level of uPAR in KO-uPA mice, the effect of the receptor blocking on neurite outgrowth would be more pronounced in the case of DRG from KO-uPA mice compared to control (WT).

After 14 days in culture, the DRG explants were stained with DAPI and antibody recognizing axons (NF200). Fig. 8 shows the confocal images of a three-dimensional immunofluorescence staining of DRG explants. It appeared that, indeed, blocking the urokinase receptor in ganglia explants from KO-uPA mice resulted in more profound adverse effects on the axon growth trajectory compared to axons growing from DRGs of wild type mice. Supplementary materials contain videos of stereomicroscopy images obtained using 3D DRG explants and are presented in Fig. 8 (Video S5 and S6 in the online version at DOI: 10.1016/j.ejcb.2016.05.003).

4. Discussion

Growth cones of regenerating peripheral neurons have to migrate through a structurally altered injury site, through infiltrating cells and modified extracellular matrix, along residual basal lamina to reinnervate their synaptic targets. To promote migration, growth cones have to secrete proteases that degrade cell–cell and cell-matrix adhesion contacts. Potential means for the growth cones would be the use of proteases, such as plasminogen activators that are capable of activating other proteases, degrading extracellular matrix and destroying adhesive contacts, thus promoting the axonal outgrowth. Plasminogen activators cleave the proenzyme plasminogen to its active form plasmin that has a broad range of substrates, including the neural cell adhesion molecule NCAM in the nervous system (Endo et al., 1998).

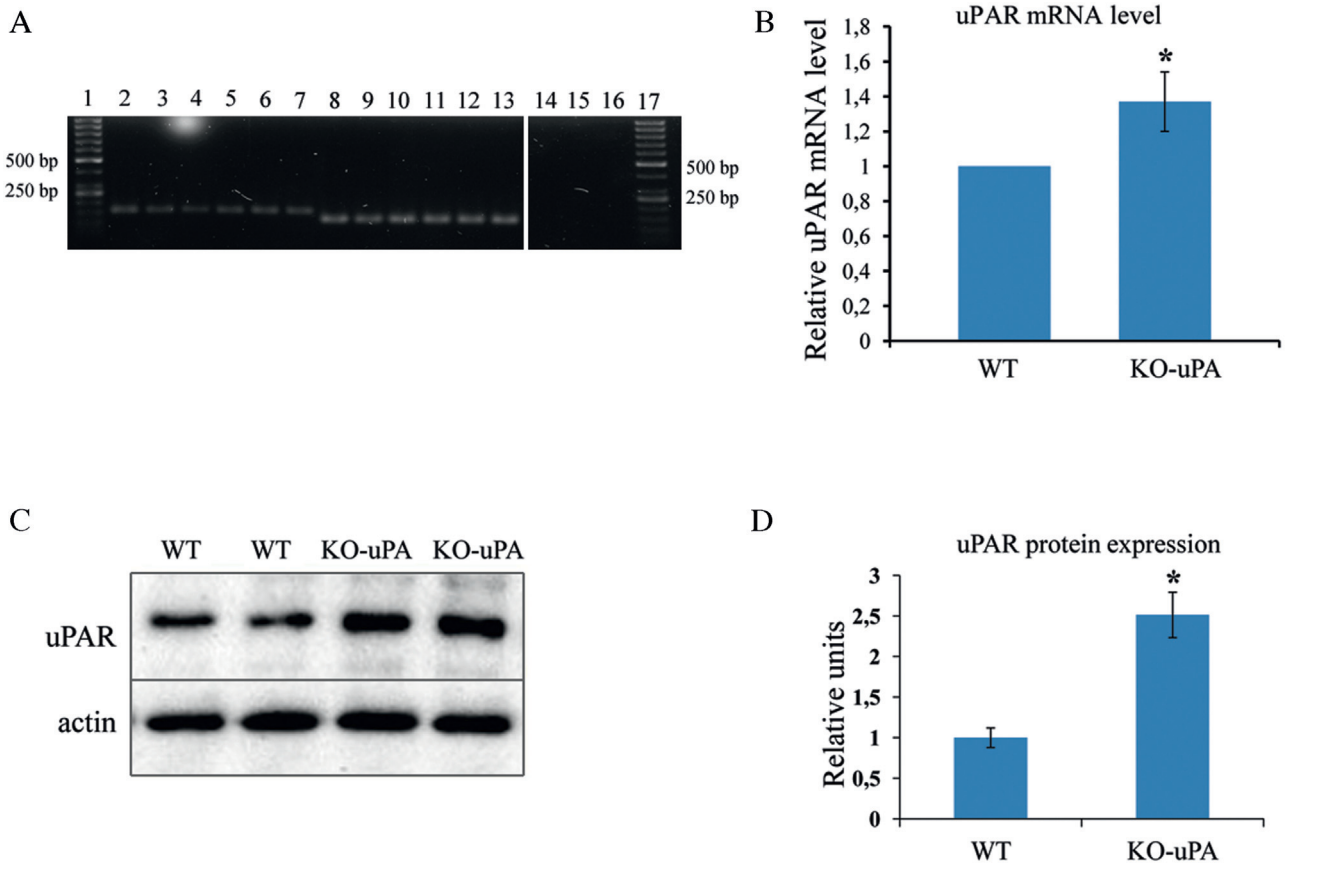

Fig. 6. uPAR expression in DRG. (A) The uPAR mRNA content in DGR explants from wild type mice (WT) and from uPA-deficient mice (KO-uPA) was evaluated using RT-PCR. Agarose gel electrophoresis after RT-PCR was carried out to verify the production of a single gene-specific product in each sample (uPAR gene (151 bp) and β-actin (112 bp)). 1, 17—DNA ladder; 2–4—probes containing WT DNA template and uPAR primers; 5–7—probes containing KO-uPA DNA template and uPAR primers; 8–10—probes containing WT DNA template and β-actin primers; 11–13—probes containing KO-uPA DNA template and β-actin primers; 14–15—negative control containing uPAR primers without DNA template; 16-—negative control containing β-actin primers without DNA template. (B) mRNA level of uPAR in DRG explants from WT and KO-uPA mice. The mRNA level of uPAR was normalized to β-actin as a housekeeping gene. Data are presented as mean ± SEM, N = 3, * $p < 0.05$. (C) Western blot analysis of uPAR expression in DRGs from WT and KO-uPA mice. Reproducible results of three independent experiments are presented. (D) Densitometry analysis of western blots results. Data are shown as mean ± SEM, N = 3, * $p < 0.05$.

It was suggested that plasminogen activators could play an important role in facilitating axon extension and cell migration during the development and regeneration of the peripheral nervous system (Pittman, 1985; Pittman et al., 1989; McGuire and Seeds, 1990; Hayden and Seeds, 1996). However, data on the potential function that the uPA/uPAR system can perform in peripheral nerves are obscure. Expression and secretion of plasminogen activators were shown to be upregulated in regenerating mammalian sensory neurons in culture (Seeds et al., 1996). The addition of plasminogen activators or plasminogen inhibitors to cultured neurons had profound effects on neurite outgrowth and cell migration (Hawkins and Seeds, 1989). In mice, after sciatic nerve crush there was an induction of mRNAs of several plasminogen activators in the sensory neurons contributing to the regeneration of the crushed nerve compared to their sham counterparts (Siconolfi and Seeds, 2001). The uPA-uPAR system was also shown to be involved in neural cell differentiation, since uPAR blocking with antibody inhibited the morphological and biochemical differentiation of PC12 cells induced by nerve growth factor NGF (Farias-Eisner et al., 2000).

In the present study, we demonstrated for the first time the essential role of uPA and uPAR in the initiation, elongation and branching of neurites. Using 3D explant culture of mouse spinal ganglia, we show that uPA and uPAR were involved in the regulation of axonal growth and branching as well as in neural cell migration (Figs. 1 and 7).

uPA exerted its effect on cell migration and neurite outgrowth via interaction with uPAR (Figs. 5C and 7). We confirmed this data *in vitro* using Neuro 2A cell culture (Figs. 4 and 5C). uPA inhibition suppressed neural cell migration and significantly abrogated axon growth rate and growth trajectory, both *ex vivo* (Fig. 1) and *in vitro* (Fig. 4), suggesting that urokinase proteolytic activity upon its interaction with uPAR is essential for these processes. However, he uPAR expression level was important for uPA-dependent stimulation of axon growth and cell migration, since in contrast to WT mice, in KO-uPA mice that exhibit elevated uPAR expression level in ganglia we observed an increased axon growth rate and neural cell migration in response to uPA administration (Fig. 7).

One would expect that blocking of uPA and uPAR interaction would affect neurite outgrowth and cell migration and the obtained data were unexpected. Indeed, uPAR blocking suppressed neural cell migration (Fig. 1) while in neurons it caused changes in cell morphology, *i.e.* an increased number of neurites and their enhanced branching (Figs. 3 and 8). Moreover, in KO-uPA mice that lacked urokinase but had an elevated level of uPAR, the observed spontaneously higher rate of neurite outgrowth suggested that uPA could be not the only ligand of uPAR (Fig. 7). It is well known that uPA can exhibit physiological effects that are independent of uPAR binding, while the uPAR function can engage multiple ligands (vitronectin, Endo180, integrins and SRPX2) (Lino et al., 2014; Engelholm et al., 2003; Wienke et al., 2007; Madsen et al., 2007; Royer-Zemmour et al., 2008; Franco et al., 2006).

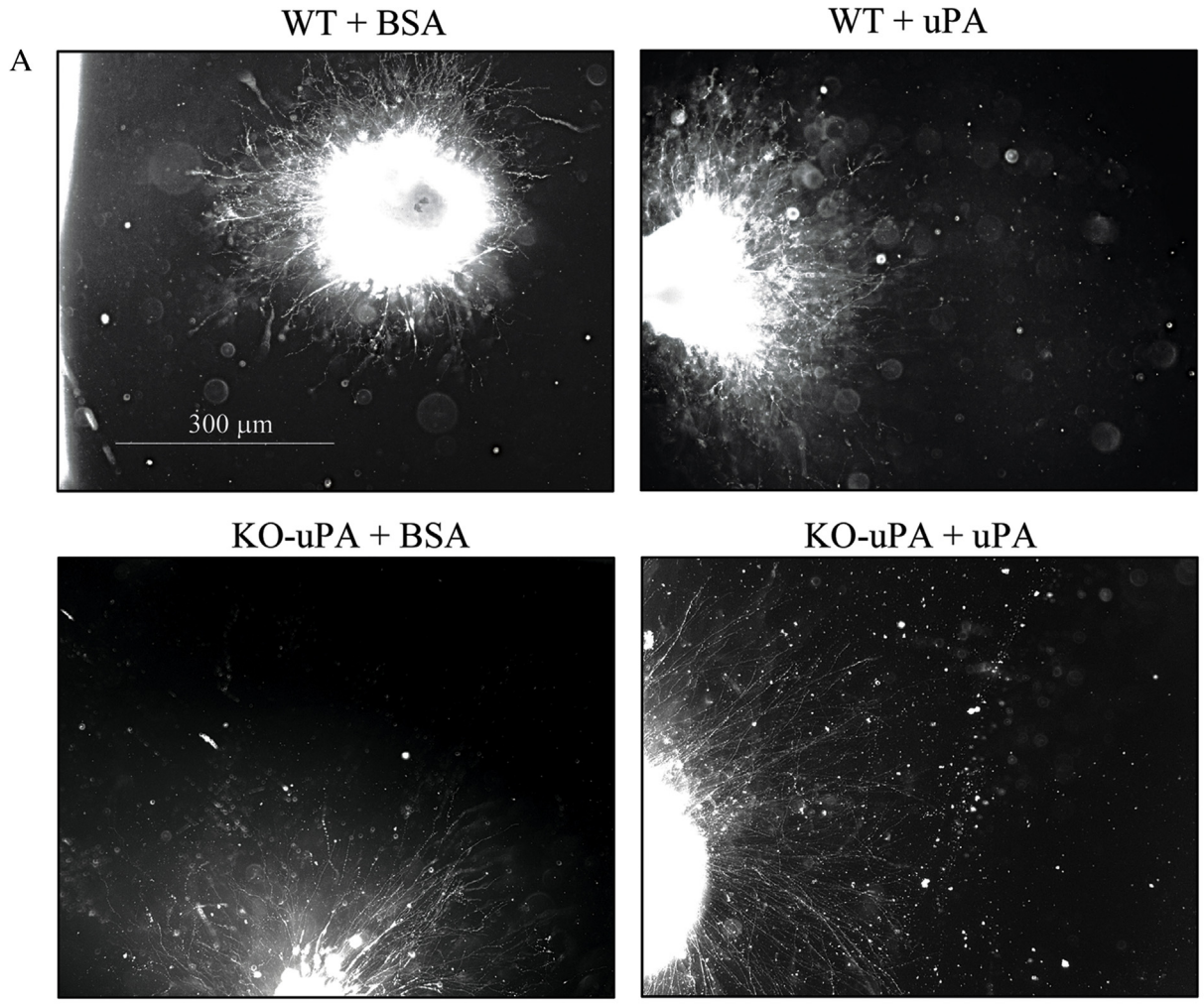

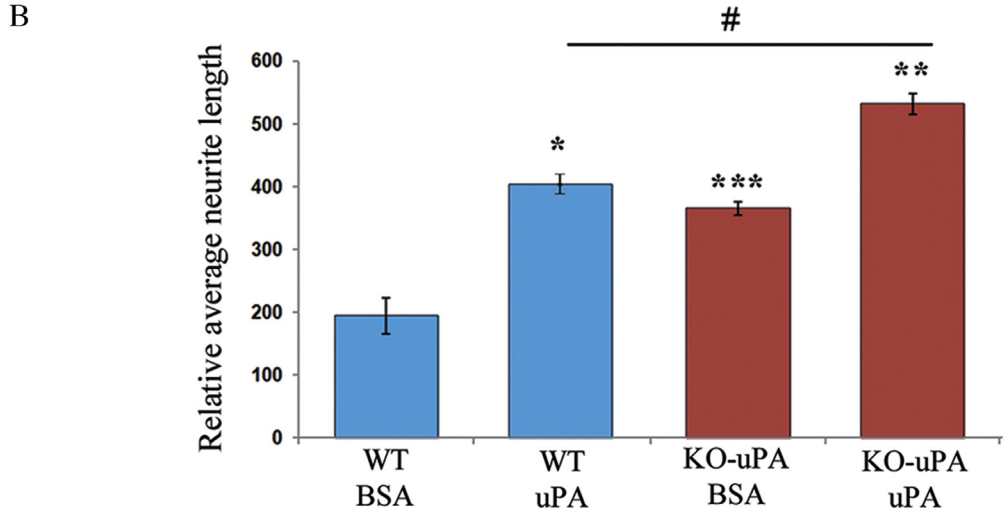

Fig. 7. uPA-uPAR interaction stimulates neurites outgrowth and neural cell migration in DGR explants. (A) DRG explants from wild type mice (WT) and mice with knockout uPA gene (KO-uPA) were cultured in the presence of uPA (10 ng/ml) or control media (BSA 10 ng/ml) for 14 days. Explants were visualized using darkfield microscopy at low magnification. Bars 300 μm. Reproducible results of three independent experiments are presented; each experiment comprises WT and KO-uPA group (4 mice in each group). (B) Calculation of the average length of neurites emerging from DGRs into Matrigels; *, $p < 0.05$ between WT + uPA and WT + BSA; **, $p < 0.05$ between KO-uPA + uPA and KO-uPA + BSA; *** $p < 0.001$ between KO-uPA + BSA and WT + BSA; # $p < 0.05$ between KO-uPA + uPA and WT + uPA. Reproducible results of three independent experiments are presented; each experiment included results from the control and the KO-uPA group (4 mice in each group). (C) DRG explants from wild type mice (WT) and mice with knockout uPA gene (KO-uPA) were cultured in the presence of uPA (10 ng/ml) or control media (BSA 10 ng/ml) during 14 days. The nuclei of migrated cells from DRG to the Matrigel were counterstained with DAPI. Dotted line indicates the border of DRG, arrows indicates the migration path of cells. Bars 300 μm. (D) Counting the number of

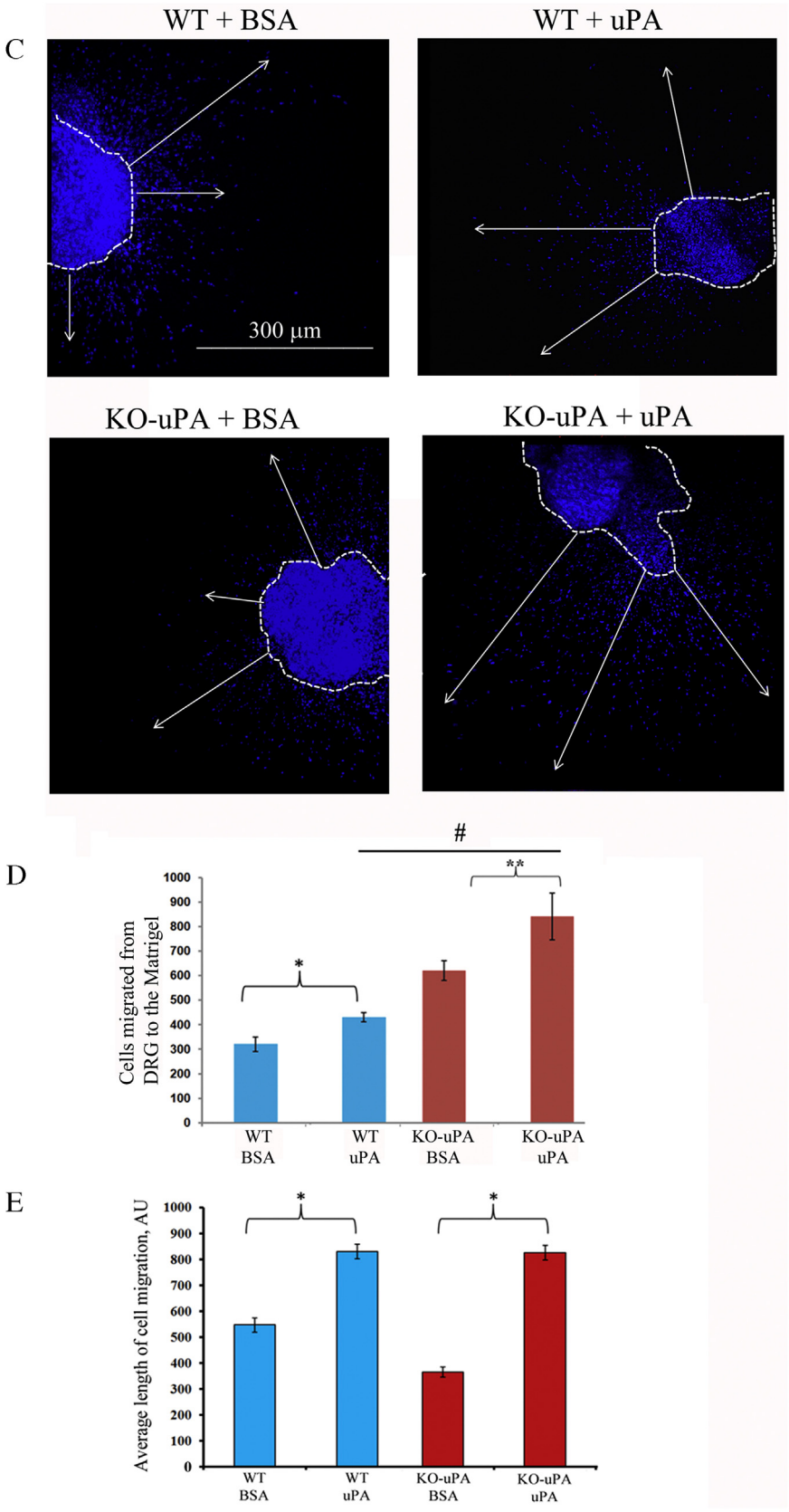

Fig. 7. (*Continued*)

cells that migrated from DGR to Matrigels (*, **, #$p < 0.05$). Reproducible results from three independent experiments using WT or KO-uPA group of animals are presented (4 mice were included in each group). (E) Evaluation of the average length of the cell migration path from DGRs into Matrigels (*, **, $p < 0.05$). Reproducible results of three independent experiments are presented; each experiment includes WT and KO-uPA group (4 mice in each group).

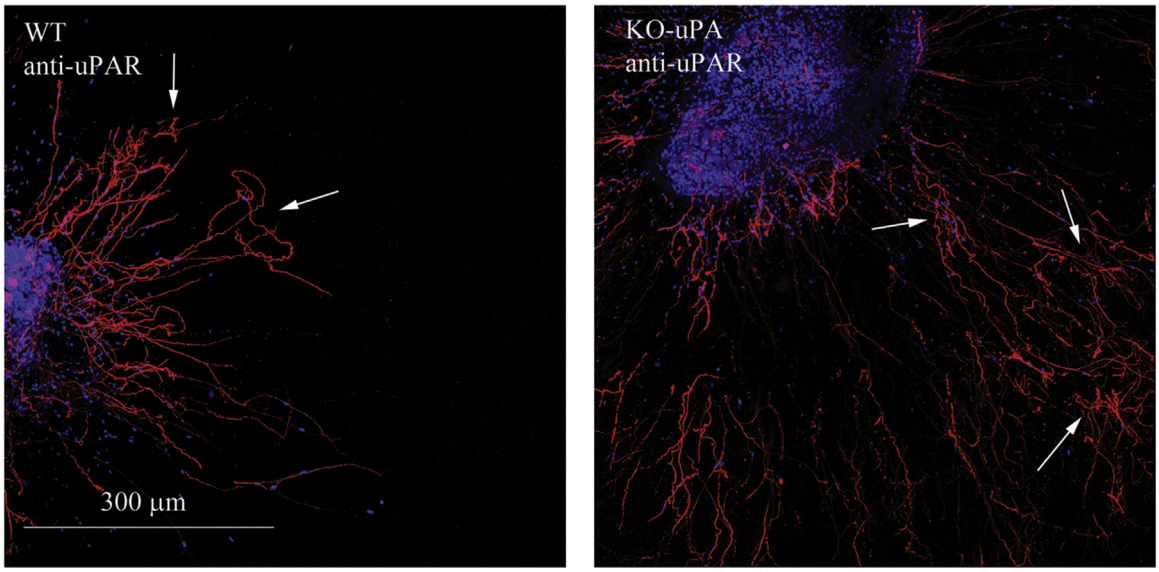

Fig. 8. uPAR blocking impairs axonal growth from DRG explants. DGR from wild type mice (WT) and mice lacking uPA gene (KO-uPA) were cultured in Matrigels containing uPAR blocking antibodies (anti-uPAR). After 14 days, DGR explants were stained with antibody against NF200 for axon visualization. The nuclei were counterstained with DAPI. uPAR blocking resulted in trajectory changes of the growing axons and their branching (arrows in the figure). Bars 300 μm. Reproducible results of three independent experiments are presented; each experiment utilized WT and KO-uPA groups of animals (3 mice were included in each group).

Upon binding to uPAR, uPA can function as a protease that degrades the extracellular matrix thus facilitating the migration of vascular cells (Blasi and Sidenius, 2010; Blasi and Carmeliet, 2002) and neural cells (Figs. 1 and 7). However, uPAR itself can function uPA-independently (Blasi and Sidenius, 2010; Blasi and Carmeliet, 2002). In the present study we describe the effects of uPAR on neuron morphology. We suggest that uPAR may function uPA-independently and these effects could be attributed to uPAR interaction with alternative ligands in the nervous system.

The assumption that uPAR could be involved in neuronal differentiation is supported by data on uPAR knockout mice. uPAR null (uPAR-/-) mice lack parvalbumin-containing GABA-interneurons neurons and are characterized by abnormalities in the developing brain cortex which are associated with increased susceptibility to spontaneous and chemically-induced seizures and with increased anxiety and impaired social interactions (Bruneau and Szepetowski, 2011; Royer-Zemmour et al., 2008). This phenotype was observed only in uPAR-/- mice, but not in uPA-/- mice, which suggests the presence of an alternative ligand of uPAR with other functions in the central nervous system. Recent studies indicate that Sushi repeat protein, X-linked 2 (SRPX2) interacts with uPAR, and inhibition of SRPX2 interaction with uPAR results in an uPAR-/-—like phenotype (Royer-Zemmour et al., 2008; Franco et al., 2006).

In axons, the appropriate interaction of cell adhesion molecules with extracellular matrix is crucial for development of nervous system. Axon growth and polarization during neurogenesis is highly dependent upon the assembly of integrin complexes. Integrins have been implicated in uPA/uPAR-dependent activation of cell adhesion and cell morphology changes in non-neuronal systems (Blasi and Carmeliet, 2002; Blasi and Sidenius, 2010; Carmeliet, 2003; Franco et al., 2006; Wei et al., 2001; Wei et al., 1996), but little is known about uPAR-integrins' interaction in neurons. It has been suggested that cooperation of uPAR and α/β integrin heterodimers is necessary for uPA-dependent neuron migration and neuritogenesis (Lino et al., 2014). It is tempting to speculate that the uPA/uPAR system, and particular uPAR, can exert its effects on the formation and regulation of axon branching via interaction with the integrin complex. However, this assumption needs further investigation.

To further investigate the role of uPA/uPAR in the neural cell migration, growth and axon branching we utilized 3D explant DRG cultures from wild type and uPA-deficient mice. Administration of exogenous uPA significantly stimulated neurite outgrowth from both, the WT and KO-uPA DRGs. It is notable that uPAR expression in ganglia from KO-uPA mice was elevated, compared to the WT mice, and that the spontaneous neurite formation (neurite length) in KO-uPA explants was higher than in WT DRGs, probably due to the elevated uPAR expression. Administration of uPA resulted in the significant stimulation of neurite outgrowth and neural cell migration from DRG of KO-uPA mice compared to the WT. Moreover, uPAR blocking dramatically affected the axonal growth pattern from DRG of KO-uPA mice compared to WT ganglia and resulted in axonal trajectory distortion. Similar effects were obtained on neural cell migration from WT and KO-uPA DRGs. The described results indicate that the urokinase system contributes significantly to neural cell migration and neuron morphology, and affects the initiation, elongation and branching of neurites.

5. Conclusion

In the present study we describe the essential role of the uPA and uPAR in axonal growth and branching, and in neural cell migration. The suppression of endogenous urokinase substantially abrogated the axonal growth by decreasing the length of axons and their total number as well as by distorting their normal growth trajectory. Moreover, uPA inhibition significantly reduced the rate and the number of cells migrating from DRG explants into Matrigels. Inhibition of uPA-uPAR interaction by anti-uPAR antibody resulted in a dramatic reduction of the total number of growing axons and the number of cells migrating from DRG explants into Matrigels. This was also characterized by alterations in the trajectory of the growing axons and their increased branching. Inhibition of both, uPA and uPAR, almost totally blocked the growth of axons from DRG explants.

It is notable that uPAR expression in ganglia obtained from mice lacking uPA (KO-uPA) was significantly increased compared to control (WT mice). The length of neurites in DRG explant culture from KO-uPA mice was greater than in control DRGs, which may be due to the elevated uPAR expression. Administration of uPA resulted in pronounced stimulation of neurite outgrowth and neural cell migration from DRG of KO-uPA mice compared to the

control. uPAR blocking led to the reduction in the number of the growing axons from DRG of KO-uPA mice compared to ganglia from WT mice. Moreover, uPAR blocking dramatically affected the axon growth pattern resulting in the distorted trajectory of the axons growing from DRG of KO-uPA mice. The obtained results indicate that the urokinase system contributes significantly to the neural cell migration, initiation, elongation and branching of neurites.

Using Neuro 2a cells differentiated into neurons, we found that blocking uPA/uPAR interactions by using uPAR-blocking antibodies stimulated neurite formation and enhanced the branching of pre-existing neurites. The addition of uPA stimulated the elongation of neurites, most likely via the interaction of uPA with its specific receptor uPAR located on the growth cones of axons. Based on the results obtained in this study, we suppose that uPA stimulates axon growth and neural cell migration by cooperation with uPAR and uPAR involved in axon formation and branching.

Competing interests

The authors have declared no conflict of interest including any financial, personal or other relationships with other people or organizations.

Author contributions

Semina Ekaterina contributed to the acquisition of data, its analysis and interpretation, Rubina Kseniya contributed to data analysis and interpretation, Sysoeva Veronika contributed to the design of the study, Rysenkova Karina and Polina Klimovich contributed to the acquisition of data, Plekhanova Olga contributed to data analysis and Tkachuk Vsevolod made a substantial contribution to the conception of the manuscript. All of the authors approved the final version of the manuscript.

Acknowledgments

Source of funding: grant (№14-24-00086) of the Russian Science Foundation. The authors acknowledge that the work was carried out using equipment purchased with funding from the Program of Development of M.V. Lomonosov Moscow State University. The team of authors is also grateful to P.N. Makarevich for assessing uPAR expression in the DRG by western blotting and to M. Kazarnovsky for assistance in statistical analysis of the length of neurites in N2a cells.

References

Blasi, F., Carmeliet, P., 2002. uPAR: a versatile signalling orchestrator. Nat. Rev. Mol. Cell Biol. 3, 932.
Blasi, F., Sidenius, N., 2010. The urokinase receptor: focused cell surface proteolysis, cell adhesion and signaling. FEBS Lett. 584, 1923.
Bruneau, N., Szepetowski, P., 2011. The role of the urokinase receptor in epilepsy, in disorders of language, cognition, communication and behavior, and in the central nervous system. Curr. Pharm. Des. 17, 1914.
Carmeliet, P., Schoonjans, L., Kieckens, L., Ream, B., Degen, J., Bronson, R., De Vos, R., van den Oord, J.J., Collen, D., Mulligan, R.C., 1994. Physiological consequences of loss of plasminogen activator gene function in mice. Nature 368, 419.
Carmeliet, P., 2003. Blood vessels and nerves: common signals, pathways and diseases. Nat. Rev. Genet. 4, 710.
Collen, D., 1999. The plasminogen (fibrinolytic) system. Thromb. Haemost. 82, 259.
Dent, M.A., Sumi, Y., Morris, R.J., Seeley, P.J., 1993. Urokinase-type plasminogen activator expression by neurons and oligodendrocytes during process outgrowth in developing rat brain. Eur. J. Neurosci. 5, 633.
Eagleson, K.L., Bonnin, A., Levitt, P., 2005. Region- and age-specific deficits in gamma-aminobutyric acidergic neuron development in the telencephalon of the uPAR(-/-) mouse. J. Comp. Neurol. 489, 449.
Endo, A., Nagai, N., Urano, T., Ihara, H., Takada, Y., Hashimoto, K., Takada, A., 1998. Proteolysis of highly polysialylated NCAM by the tissue plasminogen activator-plasmin system in rats. Neurosci. Lett. 246, 37.
Engelholm, L., List, K., Netzel-Arnett, S., Cukierman, E., Mitola, D.J., Aaronson, H., Kjoller, L., Larsen, J.K., Yamada, K.M., Strickland, D.K., Holmbeck, K., Dano, K., Birkedal-Hansen, H., Behrendt, N., Bugge, T.H., 2003. uPARAP/Endo180 is essential for cellular uptake of collagen and promotes fibroblast collagen adhesion. J. Cell Biol. 160, 1009.
Estreicher, A., Wohlwend, A., Belin, D., Schleuning, W., Vassalli, J., 1989. Characterization of the cellular binding site for the urokinase type plasminogen activator. J. Biol. Chem. 264, 1180.
Estreicher, A., Muhlhauser, J., Carpentier, J., Orci, L., Vassalli, J., 1990. The receptor for urokinase type plasminogen activator polarizes expression of the protease to the leading edge of migrating monocytes and promotes degradation of enzyme inhibitor complexes. J. Cell Biol. 111, 783.
Farias-Eisner, R., Vician, L., Silver, A., Reddy, S., Rabbani, S.A., Herschman, H.R., 2000. The urokinase plasminogen activator receptor (UPAR) is preferentially induced by nerve growth factor in PC12 pheochromocytoma cells and is required for NGF-Driven differentiation. J. Neurosci. 20, 230.
Franco, P., Vocca, I., Carriero, M.V., Alfano, D., Cito, L., Longanesi-Cattani, I., Grieco, P., Ossowski, L., Stoppelli, M.P., 2006. Activation of urokinase receptor by a novel interaction between the connecting peptide region of urokinase and alpha v beta 5 integrin. J. Cell Sci. 119, 3424.
Goncharova, E.A., Vorotnikov, A.V., Gracheva, E.O., Wang, C.L., Panettieri, R.A., Stepanova, V.V., Tkachuk, V.A., 2002. Activation of p38 MAP-kinase and caldesmon phosphorylation are essential for urokinase-induced human smooth muscle cell migration. Biol. Chem. 383, 115.
Hawkins, R.L., Seeds, N.W., 1989. Protease inhibitors influence the direction of neurite outgrowth. Brain Res. Dev. Brain Res. 45, 203.
Hayden, S.M., Seeds, N.W., 1996. Modulated expression of plasminogen activator system components in cultured cells from dissociated mouse dorsal root ganglia. J. Neurosci. 16, 2307.
Kjoller, L., Hall, A., 2001. Rac mediates cytoskeletal rearrangements and increased cell motility induced by urokinase-type plasminogen activator receptor binding to vitronectin. J. Cell Biol. 152, 1145.
Krystosek, A., Seeds, N.W., 1984. Peripheral neurons and Schwann cells secrete plasminogen activator. J. Cell Biol. 98, 773.
Krystosek, A., Verrall, S., Seeds, N.W., 1988. Plasminogen activator secretion in relation to Schwann cell activities. Int. J. Dev. Neurosci. 6, 483.
Lino, N., Fiore, L., Rapacioli, M., Teruel, L., Flores, V., Scicolone, G., Sanchez, V., 2014. uPA-uPAR molecular complex is involved in cell signaling during neuronal migration and neuritogenesis. Dev. Dyn. 243, 676.
Madsen, C.D., Maria, G., Ferraris, S., Andolfo, A., Cunningham, O., Sidenius, N., 2007. uPAR-induced cell adhesion and migration: vitronectin provides the key. J. Cell Biol. 177, 927.
McGuire, P., Seeds, N., 1990. Degradation of extracellular matrix by sensory neurons during neurite outgrowth. Neuron 4, 633.
Menshikov, M., Plekhanova, O., Cai, H., Chalupsky, K., Parfyonova, Y., Bashtrikov, P., Tkachuk, V., Berk, B.C., 2006a. Urokinase plasminogen activator stimulates vascular smooth muscle cell proliferation via redox-dependent pathways. Arterioscler. Thromb. Vasc. Biol. 26, 801.
Menshikov, M., Torosyan, N., Elizarova, E., Plakida, K., Vorotnikov, A., Parfyonova, Y., Stepanova, V., Bobik, A., Berk, B., Tkachuk, V., 2006b. Urokinase induces matrix metalloproteinase-9/gelatinase B expression in THP-1 monocytes via ERK1/2 and cytosolic phospholipase A2 activation and eicosanoid production. J. Vasc. Res. 43, 482.
Mukhina, S., Stepanova, V., Traktouev, D., Poliakov, A., Beabealashvilly, R., Gursky, Y., Minashkin, M., Shevelev, A., Tkachuk, V., 2000. The chemotactic action of urokinase on smooth muscle cells is dependent on its kringle domain. Characterization of interactions and contribution to chemotaxis. J. Biol. Chem. 275, 16450.
Ndode-Ekane, X.E., Pitkänen, A., 2013. Urokinase-type plasminogen activator receptor modulates epileptogenesis in mouse model of temporal lobe epilepsy. Mol. Neurobiol. 47, 914.
Pittman, R., Ivins, J., Buettner, H., 1989. Neuronal plasminogen activators: cell surface binding sites and involvement in neurite outgrowth. J. Neurosci. 9, 4269.
Pittman, R., 1985. Release of plasminogen activator and a calcium-dependent metalloprotease from cultured sympathetic and sensory neurons. Dev. Biol. 110, 91.
Plekhanova, O., Parfyonova, Y., Bibilashvily, R., Domogatskii, S., Stepanova, V., Gulba, D.C., Agrotis, A., Bobik, A., Tkachuk, V., 2001. Urokinase plasminogen activator augments cell proliferation and neointima formation in injured arteries via proteolytic mechanisms. Atherosclerosis 159, 297.
Plekhanova, O., Berk, B.C., Bashtrykov, P., Brooks, A.I., Tkachuk, V., Parfyonova, Y., 2009. Oligonucleotide microarrays reveal regulated genes related to inward arterial remodeling induced by urokinase plasminogen activator. J. Vasc. Res. 46, 177.
Poliakov, A.A., Mukhina, S.A., Traktouev, D.O., Bibilashvily, R.S., Gursky, Y.G., Minashkin, M.M., Stepanova, V.V., Tkachuk, V.A., 1999. Chemotactic effect of urokinase plasminogen activator: a major role for mechanisms independent of its proteolytic or growth factor domains. J. Recept. Signal Transduct. Res. 19, 939.
Royer-Zemmour, B., Ponsole-Lenfant, M., Gara, H., Roll, P., Lévêque, C., Massacrier, A., Ferracci, G., Cillario, J., Robaglia-Schlupp, A., Vincentelli, R., Cau, P., Szepetowski, P., 2008. Epileptic and developmental disorders of the speech cortex: ligand/receptor interaction of wild-type and mutant SRPX2 with the plasminogen activator receptor uPAR. Hum. Mol. Genet. 17, 3617.

Seeds, N., Friedman, G., Hayden, S., Thewke, C., Haffke, S., McGuire, P., Krystosek, A., 1996. Plasminogen activators and their interaction with the extracellular matrix in neural development, plasticity and regeneration. Semin. Neurosci. 8, 405.

Siconolfi, L.B., Seeds, N.W., 2001. Mice lacking tPA, uPA, or plasminogen genes showed delayed functional recovery after sciatic nerve crush. J. Neurosci. 21, 4348.

Stepanova, V., Mukhina, S., Kohler, E., Resink, T.J., Erne, P., Tkachuk, V.A., 1999. Urokinase plasminogen activator induces human smooth muscle cell migration and proliferation via distinct receptor-dependent and proteolysis-dependent mechanisms. Mol. Cell. Biochem. 195, 199.

Sumi, Y., Mar, D., Owen, D.E., Seeley, P.J., Morris, R.J., 1992. The expression of tissue and urokinase-type plasminogen activators in neural development suggests different modes of proteolytic involvement in neuronal growth. Development 116, 625.

Vassalli, J., Baccino, D., Belin, D., 1985. A cellular binding site for the Mr 55,000 form of the human plasminogen activator urokinase. J. Cell Biol. 100, 86.

Wei, Y., Lukashev, M., Simon, D.I., Bodary, S.C., Rosenberg, S., Doyle, M.V., Chapman, H.A., 1996. Regulation of integrin function by the urokinase receptor. Science 273, 1551.

Wei, Y., Eble, J.A., Wang, Z., Kreidberg, J.A., Chapman, H.A., 2001. Urokinase receptors promote β1 integrin function through interactions with integrin α3β1. Mol. Biol. Cell 12, 2975.

Wienke, D., Davies, G.C., Johnson, D.A., Sturge, J., Lambros, M.B., Savage, K., Elsheikh, S.E., Green, A.R., Ellis, I.O., Robertson, D., Reis-Filho, J.S., Isacke, C.M., 2007. The collagen receptor Endo180 (CD280) Is expressed on basal-like breast tumor cells and promotes tumor growth in vivo? Cancer Res. 67, 10230.